

NASA Technical Paper 1587

NASA
TP
1587
c.1

LOCATED BY
AFWL TECHNICAL
KIRTLAND AFB

TECH LIBRARY KAFB, NM
0134787

An Asymptotic Expansion Approach to the Inverse Radiative Transfer Problem

Richard I. Gomberg and James J. Buglia

DECEMBER 1979

NASA



NASA Technical Paper 1587

An Asymptotic Expansion Approach to the Inverse Radiative Transfer Problem

Richard I. Gomberg and James J. Buglia
Langley Research Center
Hampton, Virginia



National Aeronautics
and Space Administration

**Scientific and Technical
Information Branch**

1979

SUMMARY

A number of accepted techniques exist to invert radiant transfer data. Each technique involves certain assumptions and has inherent limitations. Derived here is a new iterative technique which recovers density profiles in a nonhomogeneous absorbing atmosphere. The technique is based on the concept of factoring a function of the density profile into the product of a known term and a term which is not known, but whose power series expansion can be found. This series converges rapidly under a wide range of conditions.

A demonstration example of simulated data from a high-resolution infrared heterodyne instrument is inverted. For the examples studied, the technique is shown to be capable of extracting features of ozone profiles in the troposphere and to be particularly stable.

INTRODUCTION

One of the fundamental problems in the theory of atmospheric remote sensing can be posed as follows: If the radiation emitted from an object whose emissive characteristics are known is measured in each of a number of instrument channels after the radiation has passed through an absorbing atmosphere with known or assumed optical properties, what can be inferred from these measurements about the vertical distribution of the absorbing species in the atmosphere? For example, one may want to infer the concentration profiles of an atmospheric gas or the temperature profile of the atmosphere from measurements made by an instrument looking toward the Earth from a satellite and sensing radiation emitted from the Earth in several frequency bands or at several different viewing angles.

Considerable work has been done in the field of inversion theory (refs. 1 to 5). As a result, a number of reliable techniques are available to "invert" radiant transfer data. The purpose of this paper is to derive a new iterative technique for inferring concentration profiles from such a set of measurements. In order to examine some of the convergence properties of this method, it is used to invert two numerical demonstration examples. The results are compared with those of other standard inversion techniques.

The present method is very similar to that developed by W. L. Smith (ref. 1), the difference being in the mathematical form of the "weighting functions" described herein. Although neither method is restricted to a homogeneous atmosphere, both methods reduce to the same algebraic form for the special condition of nadir viewing in a homogeneous medium.

SYMBOLS

B	Planck function
f	general function in equation (1)
g,h	general functional form
I	radiation spectral intensity
J	total number of instrument channels
K	absorption cross section
n	$n(z)$, number density
p	pressure at altitude z
p_0	sea-level pressure
S	weighting integral defined by equation (A18)
T	transmittance
U	optical mass
W	weighting function
y	$\ln (p/p_0)$
z	altitude measured from sea level
z'	variable of integration
ϵ	function defined by equation (A6)
μ	cosine of angle emerging ray makes with local vertical
τ	optical depth
ϕ	instrument response function

Subscripts:

j	channel number, 1, 2, . . . , J
TOP	top of atmosphere, or satellite altitude
λ	wavelength

Superscripts:

m	iteration number
meas	measured value
*	particular altitude in interval $[0, z_{\text{TOP}}]$

PRELIMINARY REMARKS

In the present approach, the intensity at the top of the atmosphere $I_{\lambda}(z_{\text{TOP}})$ is related to the concentration throughout the atmosphere by an equation of the form

$$I_{\lambda}(z_{\text{TOP}}, \mu) = B_{\lambda}(z_{\text{TOP}}) + \int_0^{z_{\text{TOP}}} dz' f_{\lambda}[K_{\lambda}(z'), B_{\lambda}(z'), \mu, n(z')] \quad (1)$$

in which the quantity to be determined is the vertical distribution of the absorbing species $n(z)$. If equation (1) is put into an iterative form, the difference between I_{λ} calculated using the $(m+1)$ th iteration for $n(z)$ and that using the m th iteration is

$$\begin{aligned} \Delta I_{\lambda}(z_{\text{TOP}}, \mu) &\equiv I_{\lambda}^{(m+1)}(z_{\text{TOP}}, \mu) - I_{\lambda}^{(m)}(z_{\text{TOP}}, \mu) \\ &= \int_0^{z_{\text{TOP}}} dz' \left\{ f_{\lambda}[K_{\lambda}(z'), B_{\lambda}(z'), \mu, n^{(m+1)}(z')] \right. \\ &\quad \left. - f_{\lambda}[K_{\lambda}(z'), B_{\lambda}(z'), \mu, n^{(m)}(z')] \right\} \end{aligned} \quad (2)$$

A procedure has been found for factoring the braced term so that it can be written as the product of two functions,

$$g(z, \mu) \cdot h[z, \varepsilon(z), \mu]$$

where $g(z, \mu)$ is a known function of $n^{(m)}(z)$ and $h[z, \varepsilon(z), \mu]$ is an unknown function which depends on $n^{(m+1)}(z)$, through the term $\varepsilon(z)$. It is shown in the appendix that $\varepsilon(z)$ is bounded by a small parameter for all values of z . Thus, by expanding $h[z, \varepsilon(z), \mu]$ in a power series in $\varepsilon(z)$ and retaining only the linear terms, equation (2) can be put into the form

$$\Delta I_{\lambda}(z_{\text{TOP}}, \mu) = \int_0^{z_{\text{TOP}}} dz' \varepsilon_{\lambda}(z') W_{\lambda}(z') \quad (3)$$

where $W_{\lambda}(z)$ is known and is usually referred to as the "weighting function." In this method, the weighting function $W_{\lambda}(z)$ is given by equation (A21),

$$W_{\lambda}(z) = \frac{1}{\mu} \tau_{\lambda}(z) T_{\lambda}(z, \mu) \frac{dB_{\lambda}(z)}{dz} \quad (4)$$

where τ_{λ} is the optical depth, T_{λ} is the transmittance, and B_{λ} is the Planck function.

The weighting function concept is one which is used throughout the field of inversion theory. This function varies with altitude and essentially gives the user a picture of where the information is being obtained. If, for example, the weighting function peaks in the stratosphere at a certain frequency and angle, then practically all of the measured information is coming from high altitude. If information in the troposphere is required, look for weighting functions which peak in the troposphere. As discussed in the references (refs. 1 to 5), it is important to have a reasonably good distribution of weighting function peaks with altitude. To avoid ambiguous results, it is important that the peaks overlap as little as possible.

As can be seen from equation (4), the weighting functions in the present method vary with μ and λ . The functional dependence on μ not only occurs in the factor $1/\mu$ but also in the transmission term

$$T_{\lambda}(z, \mu) = \exp[-\tau_{\lambda}(z)/\mu] \quad (5)$$

The functions $\tau_{\lambda}(z)$, $T_{\lambda}(z, \mu)$ and $B_{\lambda}(z)$ all depend on the wavelength of the radiation being measured, since these terms all depend heavily on the molecular absorbing properties of the medium of transmission.

Since the intensity at the top of the atmosphere is measured by an instrument, the quantities such as T and τ being used in the weighting functions are more appropriately thought of as averaged quantities over the band-pass ranges of the instrument channels. Thus, for the j th channel, assuming a rectangular response function

$$\left. \begin{aligned} T_j(z, \mu) &= \frac{1}{\Delta\lambda} \int_{\lambda_{\text{lower}}}^{\lambda_{\text{upper}}} \phi(\lambda) T_{\lambda}(z, \mu) d\lambda \\ \tau_j(z) &= \frac{1}{\Delta\lambda} \int_{\lambda_{\text{lower}}}^{\lambda_{\text{upper}}} \phi(\lambda) \tau_{\lambda}(z) d\lambda \end{aligned} \right\} \quad (6)$$

and so on for all wavelength dependent quantities. The width of the channel is represented by $\Delta\lambda$, with λ_{lower} and λ_{upper} representing the lower and upper wavelengths of the channel and $\phi(\lambda)$ representing the instrument response function. If a high resolution instrument is being used, T_j and T_{λ} will be reasonably interchangeable for any wavelength in the channel. The narrower the channel, the more accurate the approximation will be.

A RETRIEVAL PROCEDURE

Measurements of the radiation emanating from and passing through the atmosphere are made in several discrete channels ($j = 1, 2, \dots, J$), each with its own finite field of view, bandwidth $[\Delta\lambda_j = (\lambda_j)_{\text{upper}} - (\lambda_j)_{\text{lower}}]$, and viewing

angle with respect to the outward normal ($\cos^{-1} \mu$). The problem faced by the researcher is determining how to infer, from these measurements, a vertical profile of a trace gas which is optically active to all channels and which has a vertical distribution consistent with all of the measurements to within the measurement error. The inversion scheme presented here provides a means for accomplishing this.

The inversion scheme outlined here is derived in detail in the appendix. The procedure, suitable for use on a high-speed computer, can be reduced to the following sequence of steps:

1. Assume an initial gas profile $n^0(z)$ as a first estimate
2. In each channel, calculate the upwelling radiance at the top of the atmosphere by using equation (A2),

$$I_j^m(z_{\text{TOP}}, \mu_j) = B_j(z_{\text{TOP}}) - \int_0^{z_{\text{TOP}}} dz' \frac{dB_j(z')}{dz'} \times \exp \left[- \frac{1}{\mu_j} \int_0^{z_{\text{TOP}}} K_j(z'') n^m(z'') dz'' \right] \quad (7)$$

3. Calculate the weighting function for each channel by use of equation (A21),

$$w_j^m(z) = \frac{1}{\mu} \tau_j^m(z) T_j^m(z) \frac{dB_j(z)}{dz} \quad (8)$$

where τ_j^m is the optical depth predicted from the measurements in the j th channel on the m th iteration and T_j^m is the corresponding transmittance computed from this value of the optical depth.

4. For each data channel, calculate a new gas profile $n_j^{(m+1)}(z)$ by use of equation (A20),

$$n_j^{(m+1)}(z) = n^m(z) \left(1 + \frac{\Delta I_j^m}{S_j^m} \right) \quad (9)$$

where

$$\Delta I_j^m = [I_j^{\text{meas}}(z_{\text{TOP}}, \mu_j) - I_j^m(z_{\text{TOP}}, \mu_j)] \quad (10)$$

and S_j^m is computed from equation (A18)

$$S_j^m = \frac{1}{\mu_j} \int_0^{z_{\text{TOP}}} dz' \frac{dB_j(z')}{dz'} \tau_j^m(z') T_j^m(z') \quad (11)$$

5. The final estimate of $n(z)$ for each altitude is obtained from a weighted average of the individual profiles, given by equation (A22),

$$n^{(m+1)}(z) = \frac{\sum_{j=1}^{j_{\text{max}}} w_j^{(m+1)}(z) n_j^{(m+1)}(z)}{\sum_{j=1}^{j_{\text{max}}} w_j^{(m+1)}(z)} \quad (12)$$

There are a number of points worth discussing in connection with this algorithm. If the weighting functions are well separated with little or no overlap (which seldom happens in practice), then the best estimate for $n(z)$ in a given altitude region is that given by the channel with a nonzero weighting function in that region; that is, if the j th channel is the only one which has a nonzero weighting function at some altitude z^* , then equation (A22) reduces essentially to

$$n(z^*) = \frac{0 + 0 + \dots + n_j(z^*) \cdot w_j^m(z) + 0 + \dots}{0 + 0 + \dots + w_j^m(z^*) + 0 + \dots} = n_j(z^*) \quad (13)$$

Thus, in the altitude regions where there is some overlap of the weighting functions, the weighting procedure provides a reasonable scheme to form a physically meaningful average of the information from the contributing channels.

In step 4 of the procedure, the step size $\frac{\Delta I_j^m(z_{\text{TOP}}, \mu_j)}{S_j^m}$ is not bounded mathematically. It has been found through experience that the rate of convergence is frequently enhanced by restricting the step size to 0.5. This value is arbitrary, but it has been found through experience to be useful. Although limiting the step may require a few more iterations in some calculations, it was found expedient to approach the solution by more moderate size steps. In some calculations, limiting the step size may even prevent divergence.

It is worth repeating that this technique is closely related to that of W. L. Smith (ref. 1), as described by Seals in reference 6. The only major differences in the algorithms are as follows:

Weighting function $W_j^m(z)$ - Given in the present technique as

$$W_j(z) = \frac{1}{\mu} \tau_j^m(z) T_j^m(z) \frac{dB_j(z)}{dz} \quad (14)$$

it is given in the Smith technique (using present notation) by

$$W_j^m(z) = U^m(z) K_j(z) T_j^m(z) \frac{dB_j(z)}{dz} \quad (15)$$

where $U^m(z)$ is the optical mass path given by the m th iteration, or by Seals as

$$W_j^m(y) = \frac{\partial B_j(y)}{\partial y} \frac{\partial T_j^m(y)}{\partial y} \quad (16)$$

with $y = \ln(p/p_0)$ when p is the pressure at level y and p_0 is the pressure at sea level.

S integral - Given in the present technique by

$$S_j = \frac{1}{\mu} \int_0^{z_{TOP}} dz \tau_j^m(z) T_j^m(z) \frac{dB_j(z)}{dz} \quad (17)$$

it was given in reference 6 by

$$S_j = \int_0 U^m(y) \frac{e^y}{n^m} \frac{\partial B_j(y)}{\partial y} \left[\frac{\partial T_j^m(y)}{\partial y} \right] dy \quad (18)$$

Thus, if the Smith algorithm is already available in program form, the present algorithm can very easily be added to the program, giving the user an additional option for inverting data.

NUMERICAL EXAMPLE

The inversion simulation was performed in three major steps:

1. A study was made to find a set of narrow data channels which was appropriate for a high-resolution infrared heterodyne spectrometer and was reasonably free of the effects of interfering gases.

2. A set of synthetic "measurement data" was created using an upwelling radiance program which evaluated equation (A1) for an assumed nominal density profile of the trace gas, ozone.

3. The algorithm described in the section "A Retrieval Procedure" was then used to invert the measurement data in an attempt to recover the density profile. No measurement error was assumed in these studies.

Detailed descriptions of these steps follow.

Channel Selection

To find appropriate wavelengths and angles at which to locate the instrument channels, the 1966 U.S. Standard Atmosphere (ref. 7) and a simple absorption model were used in a study to calculate the total transmission through a homogeneous slab where pressure, temperature, and thickness are specified. This computer program, developed by R. K. Seals, Jr., of the NASA Langley Research Center and L. L. Gordley of Systems & Applied Sciences Corporation, is unpublished. It essentially calculates the monochromatic transmissivity at a number of discrete frequencies and is based on the assumption of one basic absorbing species and up to five interfering gases. Line parameters from an updated version of the McClatchey tape (ref. 8) are used. The output consists of two curves of transmittance versus wavelength - one for the basic absorber alone and one for the basic absorber plus the interfering gases. An example of this output is shown in figure 1 for the wave-number range of 1041.5 cm^{-1} to 1044.0 cm^{-1} and in figure 2 for the range of 1050 cm^{-1} to 1060 cm^{-1} . In both figures, the basic absorbing gas was ozone and the interfering gases were carbon dioxide, water vapor, and methane. (See table I.) The water vapor continuum was not included in this model.

Several regions of minimum interference can easily be seen in these figures. To take advantage of these regions, the five channels shown in table II were chosen for the simulated soundings.

Synthetic Data

An upwelling-radiance program was developed to solve equation (A1) for a large number of monochromatic frequencies. The results were then integrated over the finite bandwidth of each channel to produce the "measurements." A rectangular instrument response function was assumed. The neutral composition of the atmosphere used is presented in table III.

In evaluating equation (A1), a plane-parallel atmosphere was used. This was broken into 50 layers, each of 2-km thickness. The Lorentz profile was used to compute the absorption cross section below an altitude of 34 km, and the Voigt profile, calculated from the computational algorithm of reference 9, was assumed above this altitude.

Inversion

With the atmospheric upwelling-radiance program, all pertinent physical variables, such as optical depth and transmissivity, can be calculated separately for each species at each altitude and wavelength. After ozone was chosen for the gas to be profiled, several instrument channels were selected. The weighting functions for these channels were computed by equation (A21) and are pictured in figure 3. Note that peaks occur below the ozone bulge at 21 km (fig. 3). The dependence on $1/\mu$ is evident in channels 3 and 5 where the same wavelength was chosen, but different angles were used. Channel 3 peaks at a slightly higher altitude, since its ratio of optical depth to μ is greater than that of channel 5 at all nonzero optical depths.

A number of profile retrievals were made corresponding to different initial guesses of the ozone profile. Two estimated profiles are shown in figure 4. After some experience was gained, it became apparent that an interesting feature of the technique presented herein was its stability, particularly in comparison with the closely related formulation of the technique of Smith in reference 6. However, it must be emphasized that, for the application of the present technique, the channel selection was made to spread the peaks of the weighting functions (eq. (A21)) as evenly as possible over the altitude range. These channels would not necessarily be suitable for the application of the Smith technique which used the weighting functions of reference 6. These weighting functions, for the same set of conditions as stated above, are shown in figure 5. These all peak above the troposphere for the stated conditions and hence all provided "information" from the same region of the atmosphere. It is possible that a more nearly optimum selection of channels tailored to the Smith weighting function would yield results similar to those obtained by the present method. The following comparison of numerical results should, therefore, be viewed as an application of both methods to the same instrument and not as a comparison of optimum retrieval techniques.

The three ozone profiles used to simulate the radiance measurements for each of the five channels are shown in figure 4. The curve labeled "First Guess for Case 1" is the initial profile used in both the present and the Smith retrieval methods. The results of the retrieved profiles are shown in figure 6. The solid line shows the true profiles, the dashed lines show the results of the present method after 30 and 54 iterations, while the dotted line shows the results of the Smith technique after 63 iterations. The present method recovers the profile below the tropopause reasonably well and does not fare too badly in recovering the bulge and the trailing profile above the tropopause. There was no substantial improvement after 30 iterations, possibly due to accumulation of round-off error (ref. 2). Using the same data, the Smith technique failed to achieve low residual values in its iterations. The residual error in this simulation is defined to be

$$\text{Residual}^m = \sum_{\text{channels}} (\text{Measured Radiance}_j - \text{Calculated Radiance}_j^m)^2$$

The residuals from both methods are shown in figure 7. Those from the present method varied quite smoothly and stabilized at about 41 iterations.

The Smith residuals also seemed to stabilize somewhat at this point, at a level about an order of magnitude higher than those of the present method. The initial rate of convergence is about the same for both methods up to about 15 iterations.

It is worth emphasizing that, for initial guesses this far from the true value, the limitation of the maximum step size to $|\Delta I/S| \leq 0.5$ was mandatory. Neither the Smith technique nor the present method converged without the use of this criterion. Negative number densities and extremely large radiances resulted when the step size was allowed to vary without bound.

The results just discussed were for a retrieval where the initial profile underestimated the true atmospheric profile at all altitudes. A profile retrieval using the present method is shown in figure 8. The initial profile has the same shape as the true profile, but everywhere overestimates the profile as shown in figure 4. The retrieved results are shown in figure 8 for the 38th iteration, and the residuals are shown in figure 9. The step size inhibition was used. Once again the present results reproduced the true profile (fig. 8) reasonably well, particularly below the tropopause. The initial behavior of the residuals was more erratic, but they eventually smoothed out and reached a value slightly higher than that of the initial profile.

CONCLUDING REMARKS

In this study a new iterative technique is derived which is capable of efficiently inferring density profiles from radiant intensity measurements made in a nonhomogeneous absorbing atmosphere at an arbitrary angle with the outward normal. Stability has been demonstrated for the examples presented, and experience indicates that the technique converges over a wide range of conditions. Instrument channels were selected to take advantage of the characteristics of high-resolution infrared heterodyne spectrometers which are capable of extracting information about ozone profiles well below the 21-km density profile bulge.

Langley Research Center
National Aeronautics and Space Administration
Hampton, VA 23665
November 19, 1979

APPENDIX

A DERIVATION OF THE RETRIEVAL ALGORITHM

In the present derivation, the assumption is made that the temperature distribution through the atmosphere, as well as the density distribution of all optically active species other than the one under investigation, is known. Under conditions of thermodynamic equilibrium for a nonscattering planar atmosphere, the radiant transfer equation for a single absorbing species relates the intensity of radiation in channel j to altitude z as follows:

$$I_j(z_{TOP}, \mu_j) = B_j(0, \mu_j) \exp\left[-\frac{1}{\mu_j} \int_0^{z_{TOP}} K_j(z') n(z') dz'\right] + \frac{1}{\mu_j} \int_0^{z_{TOP}} dz' B_j(z') \times K_j(z') n(z') \exp\left[-\frac{1}{\mu_j} \int_{z'}^{z_{TOP}} K_j(z'') n(z'') dz''\right] \quad (A1)$$

where the only sources of radiation are the Earth (which is assumed to radiate as a black body) and the atmosphere.

Integration of the second term of equation (A1) by parts yields

$$I_j(z_{TOP}, \mu_j) = B_j(z_{TOP}, \mu_j) - \int_0^{z_{TOP}} dz' \frac{dB_j(z')}{dz'} \exp\left[-\frac{1}{\mu_j} \int_{z'}^{z_{TOP}} K_j(z'') n(z'') dz''\right] \quad (A2)$$

If equation (A2) is considered to be the equation governing the intensity of the m th step of an iterative solution for $n(z)$, the difference between the intensity functions for the m th and $(m+1)$ th iteration is

$$I_j^{(m+1)} - I_j^m = - \int_0^{z_{TOP}} dz' \frac{dB_j(z')}{dz'} \left\{ \exp\left[-\frac{1}{\mu_j} \int_{z'}^{z_{TOP}} K_j(z'') n^{(m+1)}(z'') dz''\right] - \exp\left[-\frac{1}{\mu_j} \int_{z'}^{z_{TOP}} K_j(z'') n^m(z'') dz''\right] \right\} \quad (A3)$$

APPENDIX

Define the optical depth $\tau_j(z)$ at altitude z by the relation

$$\tau_j^m(z) = \int_z^{z_{TOP}} K_j(z') n^m(z') dz' \quad (A4)$$

and substitute this into equation (A3). As usual in iterative methods, the assumption is made that number $I_j^{(m+1)}$ (the radiation at the top of the atmosphere in the j th channel of the iteration following the m th) can be replaced by the value of the intensity in the j th channel as measured by the instrument. Thus,

$$\begin{aligned} \Delta I_j^m \equiv I_j^{meas}(z_{TOP}, \mu_j) - I_j^m(z_{TOP}, \mu_j) &= - \int_0^{z_{TOP}} dz' \frac{dB_j(z')}{dz'} \\ &\times \left(\exp\left\{[-\tau_j^{(m+1)}(z')]/\mu_j\right\} \right. \\ &\left. - \exp\left\{[-\tau_j^m(z')]/\mu_j\right\} \right) \end{aligned} \quad (A5)$$

Define the function $\epsilon_j^m(z)$ such that

$$\frac{\tau_j^{(m+1)}(z)}{\tau_j^m(z)} = 1 + \epsilon_j^m(z) \quad (A6)$$

Then the expression in parentheses in equation (A5) can be simplified to

$$\begin{aligned} &\exp\left\{-\tau_j^m(z') [1 + \epsilon_j^m(z')]/\mu_j\right\} - \exp[-\tau_j^m(z')/\mu_j] \\ &= \exp\left\{[-\tau_j^m(z')]/\mu_j\right\} \left(\exp\left\{[-\epsilon_j^m(z') \tau_j^m(z')]/\mu_j\right\} - 1 \right) \end{aligned} \quad (A7)$$

After completion of the m th iteration, equation (A7) reduces to the product of two terms. The first term, $\exp\left\{[-\tau_j^m(z')]/\mu_j\right\}$, is completely determined. The second term, containing the parameter $n^{(m+1)}(z)$, is unknown, but its power series expansion will converge rapidly if $[\tau_j^m(z')]/\mu_j$ is bounded and if $\epsilon_j^m(z')$ can be shown to be small enough throughout $0 \leq z' < z_{TOP}$ such that

APPENDIX

$$\left\{ \left[\epsilon_j^m(z') \tau_j^m(z') \right] / \mu_j \right\} \ll 1 \quad (\text{A8})$$

It has been found through experience (e.g., in the numerical demonstrations presented in the body of this paper) that $\epsilon_j^m(z)$ is of the order of 10^{-2} or 10^{-3} and becomes even smaller as $\Delta I^m \rightarrow 0$. Thus, since the product of $\epsilon\tau$ must be small, optical depths in excess of 10 are routinely within the range of validity of this approach.

By making the power series expansion and retaining linear terms, the right-hand side of equation (A7) can be written as:

$$\left\{ \left[-\epsilon_j^m(z') \tau_j^m(z') \right] / \mu_j \right\} \exp \left\{ \left[-\tau_j^m(z') \right] / \mu_j \right\} \quad (\text{A9})$$

Use of equation (A9) results in equation (A5) reducing to

$$\Delta I_j^m = \frac{1}{\mu_j} \int_0^{z_{\text{TOP}}} dz' \frac{dB_j(z')}{dz'} \epsilon_j^m(z') \tau_j^m(z') T_j^m(z') \quad (\text{A10})$$

where

$$T_j^m(z) \equiv \exp[-\tau_j^m(z)/\mu_j]$$

In order to show that $\epsilon_j^m(z)$ is indeed "small," and to justify further manipulation of equation (A10), the central assumption is made that the $\tau_j^m(z)$ converge uniformly on the interval $0 \leq z < z_{\text{TOP}}$ as $m \rightarrow \infty$. With this assumption, the algorithm can be derived.

That $\epsilon_j^m(z)$ is arbitrarily small on the interval $0 \leq z < z_{\text{TOP}}$ follows from rewriting equation (A6) as

$$\frac{\tau_j^{(m+1)}(z) - \tau_j^m(z)}{\tau_j^m(z)} = \epsilon_j^m(z) \quad (\text{A11})$$

Since $\tau_j^m(z)$ converges uniformly on $[0, z_{\text{TOP}}]$, this implies that there exists an integer N such that for all m larger than N and for all z contained in the interval $[0, z_{\text{TOP}}]$,

$$|\tau_j^{(m+1)}(z) - \tau_j^m(z)| < \delta'$$

APPENDIX

for a δ' still to be determined. Since $z < z_{\text{TOP}}$, $\tau_j^m(z) > 0$. Consider any $\gamma > 0$. By defining $\delta' = \gamma \tau_j^m(z^*)$ where $\tau_j^m(z^*)$ is the maximum value of $\tau_j^m(z)$ on $[0, z_{\text{TOP}}]$, then $\epsilon_j^m(z) < \gamma$ for any γ provided N is sufficiently large.

The uniform convergence of $\tau_j^m(z)$ will also be used to show that equation (A10) can be rewritten (with an arbitrarily small error as $m \rightarrow \infty$) as follows:

$$\begin{aligned} \Delta I_j^m &= \frac{1}{\mu_j} \int_0^{z_{\text{TOP}}} dz' \frac{dB_j(z')}{dz'} \epsilon_j^m(z') \tau_j^m(z') T_j^m(z') \\ &= \frac{\epsilon_j^m(z)}{\mu_j} \int_0^{z_{\text{TOP}}} dz' \frac{dB_j(z')}{dz'} \tau_j^m(z') T_j^m(z') + \Delta(z) \end{aligned} \quad (\text{A12})$$

where $\Delta(z)$ is the error created by bringing $\epsilon(z')$ outside the integral and will be shown to be arbitrarily small for all values of z in $[0, z_{\text{TOP}}]$ (and can be neglected for computational purposes).

Consider the difference

$$\Delta(z) = \frac{1}{\mu_j} \int_0^{z_{\text{TOP}}} dz' \frac{dB_j(z')}{dz'} \tau_j^m(z') T_j^m(z') [\epsilon_j^m(z') - \epsilon_j^m(z)] \quad (\text{A13})$$

where $\mu_j \neq 0$, $dB_j(z')/dz'$, $\tau_j^m(z')$, $T_j^m(z')$ are all physical quantities and are hence bounded so that

$$\frac{1}{\mu_j} \left| \frac{dB_j}{dz} \tau_j^m T_j^m \right| < M$$

$$0 \leq z < z_{\text{TOP}}$$

for some M . Thus,

$$\Delta(z) < \int_0^{z_{\text{TOP}}} dz' M [\epsilon_j^m(z') - \epsilon_j^m(z)] \quad (\text{A14})$$

But since it has just been shown that for any \bar{z} in the interval $[0, z_{\text{TOP}}]$,

$$\epsilon_j^m(\bar{z}) < \gamma \text{ for arbitrary } \gamma > 0$$

if m is sufficiently large. For $\epsilon_j^m(z')$, choose $\gamma = \delta/Mz_{\text{TOP}}$. For $\epsilon_j^m(z)$, choose $\gamma = \delta/2Mz_{\text{TOP}}$. Then,

APPENDIX

$$\Delta(z) < \int_0^{z_{\text{TOP}}} dz' M \frac{\delta}{2Mz_{\text{TOP}}} = \frac{\delta}{2} \quad (\text{A15})$$

Since δ is arbitrary, equation (A10) can be rewritten as

$$\Delta I_j^m = \frac{\epsilon_j^m(z)}{\mu_j} \int_0^{z_{\text{TOP}}} dz' \frac{dB_j(z')}{dz'} \tau_j^m(z') T_j^m(z') \quad (\text{A16})$$

with negligible error.

For any z , then

$$\Delta I_j^m = \frac{\tau_j^{(m+1)}(z) - \tau_j^m(z)}{\tau_j^m(z)} S_j^m \quad (\text{A17})$$

where

$$S_j^m = \frac{1}{\mu_j} \int_0^{z_{\text{TOP}}} dz' \frac{dB_j(z')}{dz'} \tau_j^m(z') T_j^m(z') \quad (\text{A18})$$

Thus,

$$\tau_j^{(m+1)}(z) = \tau_j^m(z) \left(1 + \frac{\Delta I_j^m}{S_j^m} \right) \quad (\text{A19})$$

By differentiating equation (A19) with respect to z and using equation (A4) to eliminate the derivative, this can be put into the form of an iterative algorithm for the number density $n(z)$,

$$n_j^{(m+1)}(z) = n_j^m(z) \left(1 + \frac{\Delta I_j^m}{S_j^m} \right) \quad (\text{A20})$$

The integrand of S_j in equation (A18) is the weighting function

$$W_j^m(z) = \frac{1}{\mu_j} \tau_j^m(z) T_j^m(z, \mu) \frac{dB_j(z)}{dz} \quad (\text{A21})$$

APPENDIX

With these weighting functions, the average $n(z)$ can be defined as

$$n^{(m+1)}(z) = \frac{\sum_{j=1}^{j_{\max}} w_j^{(m+1)}(z) n_j^{(m+1)}(z)}{\sum_{j=1}^{j_{\max}} w_j^{(m+1)}(z)} \quad (A22)$$

In the iterative algorithm described in the text, the average $n(z)$ will be used in equation (A20) rather than $n_j(z)$. This represents a physically reasonable interpolation scheme between altitudes with weighting function peaks. It should be noted that since ΔI_j^m and S_j^m are height independent, equation (A20) acts to alter the magnitude of $n(z)$, but not its profile shape. Equation (A22) does all the profile shape alteration.

REFERENCES

1. Smith, W. L.: Iterative Solution of the Radiative Transfer Equation for the Temperature and Absorbing Gas Profile of an Atmosphere. Appl. Opt., vol. 9, no. 9, Sept. 1970, pp. 1993-1999.
2. Chahine, Moustafa T.: A General Relaxation Method for Inverse Solution of the Full Radiative Transfer Equation. J. Atmos. Sci., vol. 29, no. 4, May 1972, pp. 741-747.
3. Rodgers, C. D.: Retrieval of Atmospheric Temperature and Composition From Remote Measurements of Thermal Radiation. Rev. Geophys. & Space Phys., vol. 14, no. 4, Nov. 1976, pp. 609-624.
4. Twomey, Sean: On the Deduction of the Vertical Distribution of Ozone by Ultraviolet Spectral Measurements From a Satellite. J. Geophys. Res., vol. 66, no. 7, July 1961, pp. 2153-2162.
5. Westwater, Ed R.; and Strand, Otto Neall: Statistical Information Content of Radiation Measurements Used in Indirect Sensing. J. Atmos. Sci., vol. 25, no. 5, Sept. 1968, pp. 750-758.
6. Seals, R. K., Jr.: Analysis of Tunable Laser Heterodyne Radiometry: Remote Sensing of Atmospheric Gases. AIAA J., vol. 12, no. 8, Aug. 1974, pp. 1118-1122.
7. U.S. Standard Atmosphere Supplements, 1966. Environ. Sci. Serv. Admin., NASA, and U.S. Air Force.
8. McClatchey, R. A.; Benedict, N. S.; Clough, S. A.; Bursh, D. E.; Calfee, R. F.; Fox, K.; Rothman, L. S.; and Garing, J. S.: AFCRL Atmospheric Absorption Line Parameters Compilation. AFCRL-TR-73-0096, U.S. Air Force, Jan. 1973. (Available from DDC as AD 762 904.)
9. Pierluissi, Joseph H.; Vanderwood, Peter C.; and Gomez, Richard B.: Fast Computational Algorithm for the Voigt Profile. J. Quant. Spectros. & Radiat. Transfer, vol. 18, no. 5, Nov. 1977, pp. 555-558.

TABLE I.- HOMOGENEOUS SLAB USED AS BASIS FOR SELECTING ABSORPTION CHANNELS

Path length	70 km
Pressure	50 kPa
Temperature	240 K
Composition:	
O ₃	0.1140 ng/cm ³
CO ₂	97.20 ng/cm ³
H ₂ O	120.0 ng/cm ³
NH ₃	0.5720 pg/cm ³

TABLE II.- CHANNELS SELECTED FOR SAMPLE CALCULATIONS

Channel, j	Initial wavelength, cm ⁻¹	Final wavelength, cm ⁻¹	μ_j
1	1042.20	1042.23	1
2	1041.87	1041.90	1
3	1041.58	1041.61	.707
4	1050.85	1050.88	.500
5	1041.58	1041.61	.500

TABLE III.- PROPERTIES OF ATMOSPHERE

(a) Physical

Altitude, km	Temperature, K	Pressure, Pa	Density, kg/m ³
99	185.86	0.0361	0.601×10^{-6}
95	176.59	.0706	1.26×10^{-6}
91	167.32	.138	2.63×10^{-6}
87	165.06	.299	21.9×10^{-6}
83	168.70	.667	45.7×10^{-6}
79	178.50	1.45	23.2×10^{-6}
75	196.10	2.99	43.3×10^{-6}
71	213.70	5.70	76.0×10^{-6}
67	231.70	10.39	$.128 \times 10^{-3}$
63	246.90	18.20	$.212 \times 10^{-3}$
59	259.54	30.94	$.345 \times 10^{-3}$
55	269.30	51.53	$.560 \times 10^{-3}$
51	274.42	84.17	$.909 \times 10^{-3}$
47	273.15	137.26	1.50×10^{-3}
43	264.95	226.24	2.60×10^{-3}
39	255.05	380.18	4.63×10^{-3}
35	245.15	652.55	8.77×10^{-3}
31	235.75	1 145.57	15.7×10^{-3}
27	227.50	2 054.87	29.2×10^{-3}
23	222.80	3 753.08	55.0×10^{-3}
19	218.00	6 947.86	.104
15	215.70	13 030.40	.195
11	228.90	24 267.30	.365
7	254.70	42 047.70	.590
3	279.20	71 069.40	.909
1	289.70	90 240.00	1.112

TABLE III.- Concluded

(b) Number density of absorbing species

Altitude, km	H ₂ O, molecules/m ³	O ₃ , molecules/m ³
99		
95	4.519×10^{13}	8.623×10^{11}
91	8.228×10^{13}	2.104×10^{12}
87	1.497×10^{14}	5.136×10^{12}
83	2.883×10^{14}	1.336×10^{13}
79	5.654×10^{14}	3.740×10^{13}
75	1.100×10^{15}	1.035×10^{14}
71	2.096×10^{15}	2.959×10^{14}
67	3.992×10^{15}	8.459×10^{14}
63	8.248×10^{15}	2.029×10^{15}
59	1.751×10^{16}	4.591×10^{15}
55	3.773×10^{16}	1.021×10^{16}
51	8.061×10^{16}	2.162×10^{16}
47	1.740×10^{17}	4.576×10^{16}
43	3.754×10^{17}	1.085×10^{17}
39	8.093×10^{17}	2.674×10^{17}
35	1.781×10^{18}	6.164×10^{17}
31	4.174×10^{18}	1.162×10^{18}
27	9.780×10^{18}	2.192×10^{18}
23	1.293×10^{19}	3.013×10^{18}
19	1.412×10^{19}	3.726×10^{18}
15	2.478×10^{19}	3.827×10^{18}
11	1.797×10^{20}	2.251×10^{18}
7	1.304×10^{21}	1.324×10^{18}
3	1.078×10^{22}	1.025×10^{18}
1	9.309×10^{22}	8.707×10^{17}
	2.735×10^{23}	8.022×10^{17}

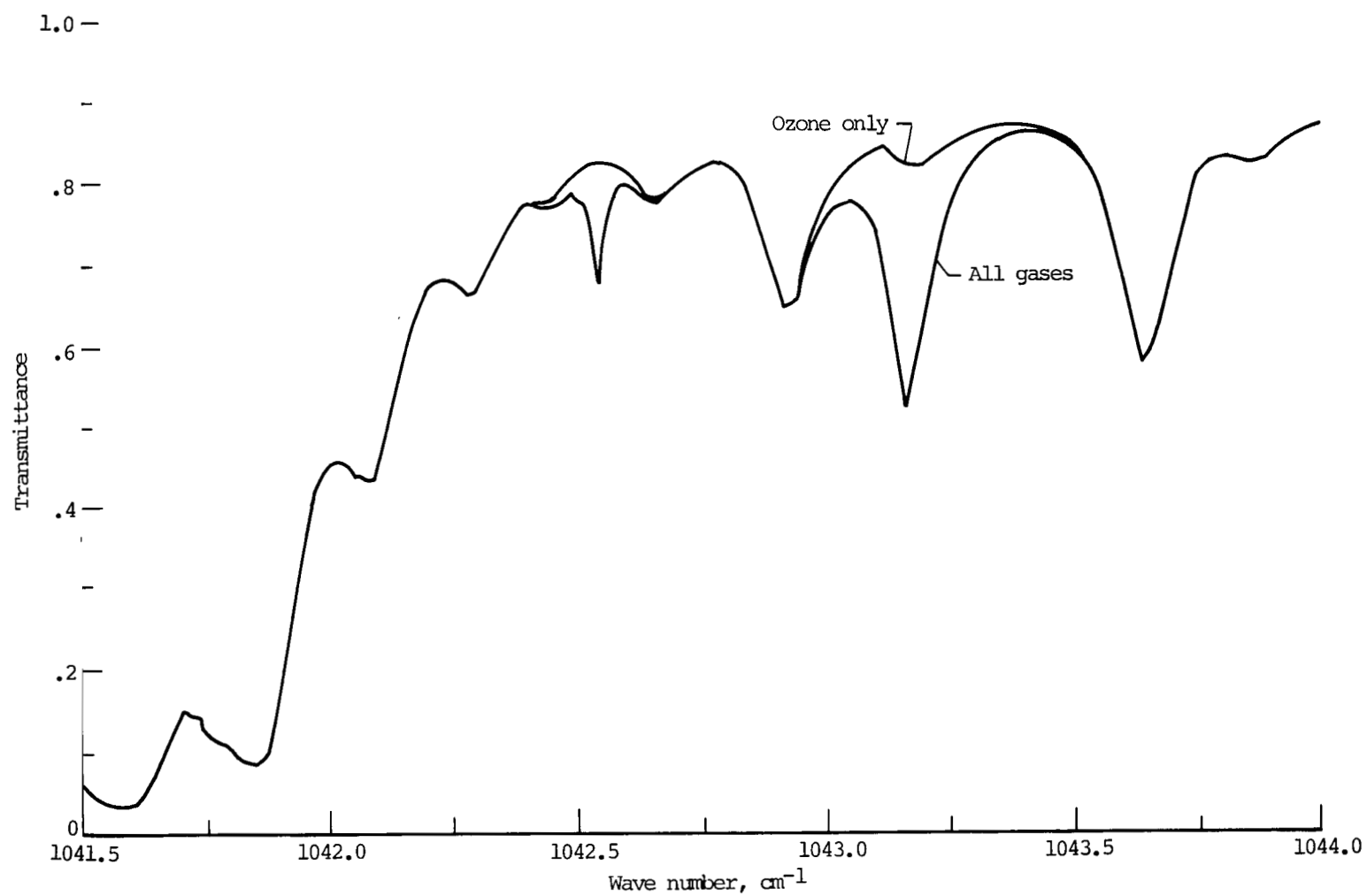


Figure 1.- Transmittance as function of wave number for homogeneous slab from 1041.5 to 1044.0 cm^{-1} .

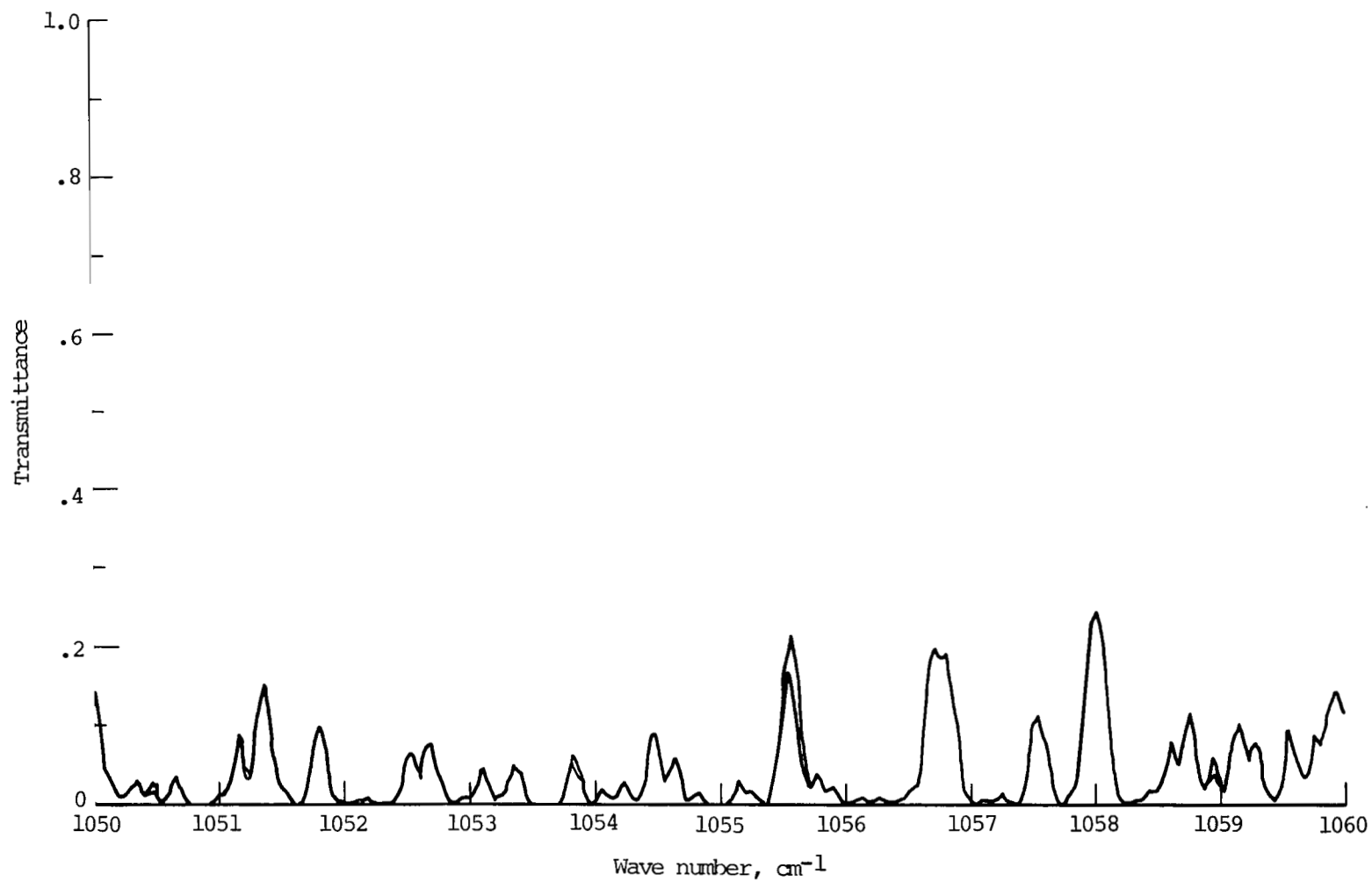


Figure 2.- Transmittance as function of wave number for homogeneous slab from 1050 to 1060 cm⁻¹.

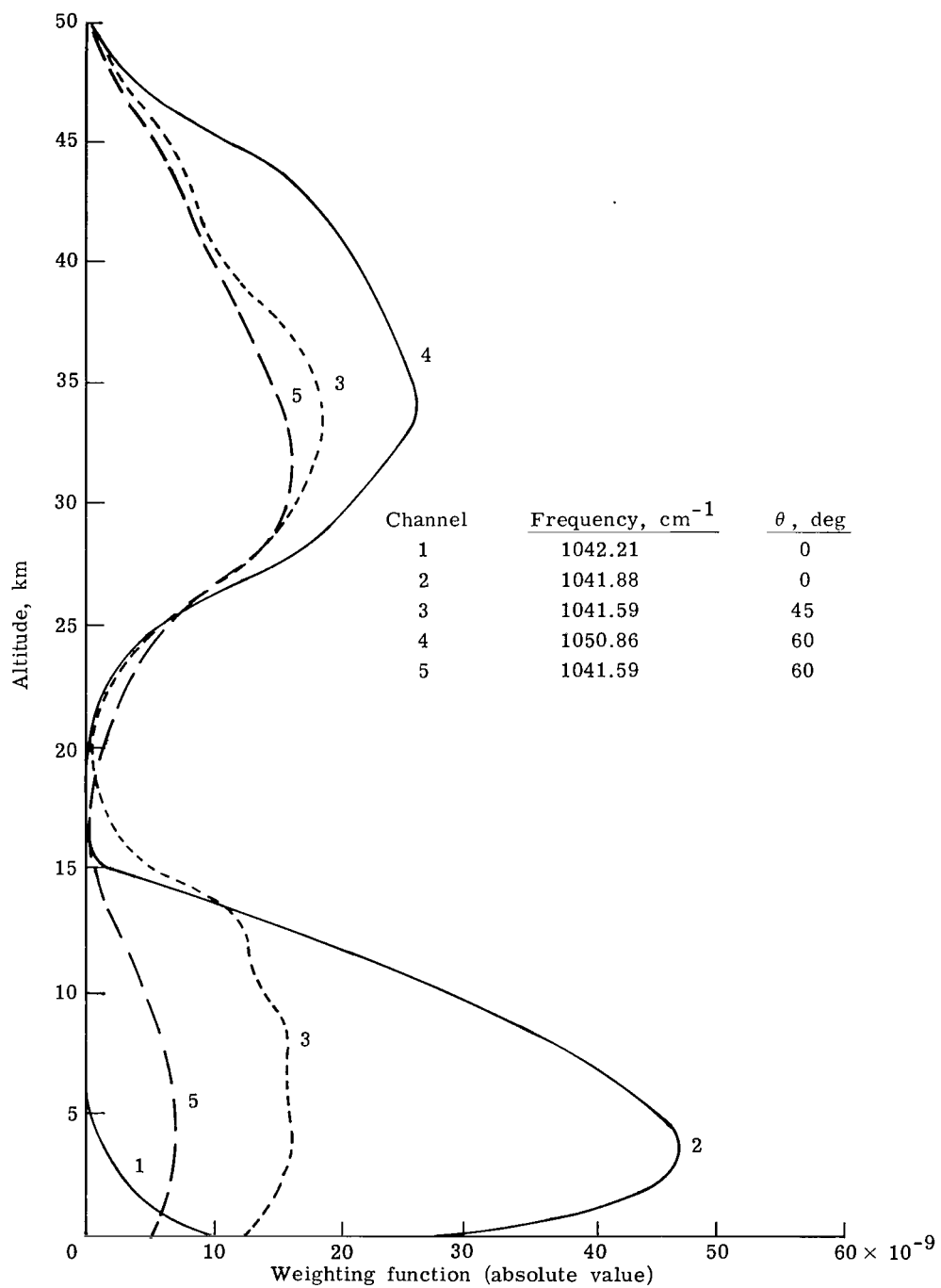


Figure 3.- Set of weighting functions for ozone determined by present method.

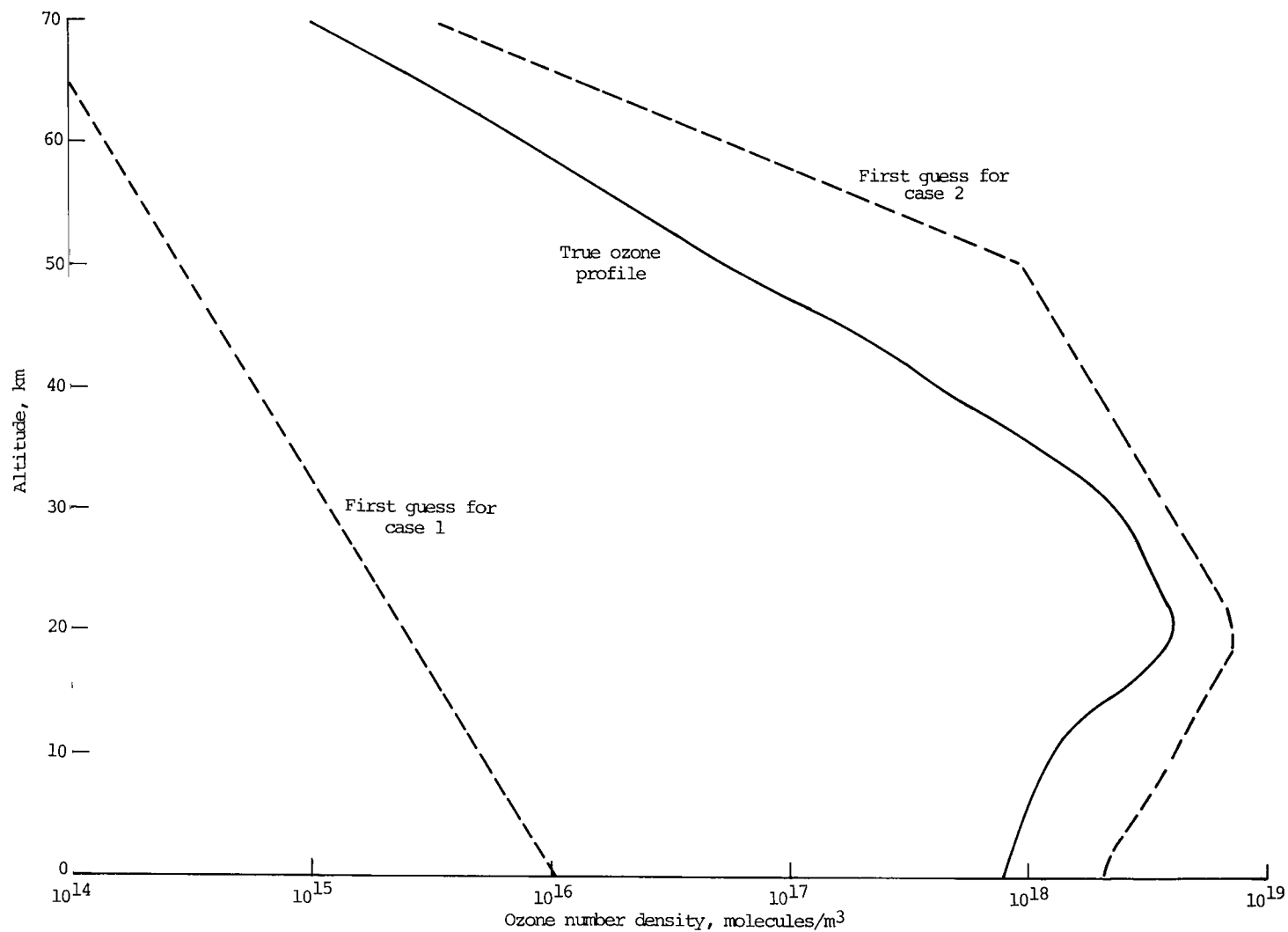


Figure 4.- Three ozone profiles used in present study. "First guess" curves were starting points for iterative scheme.

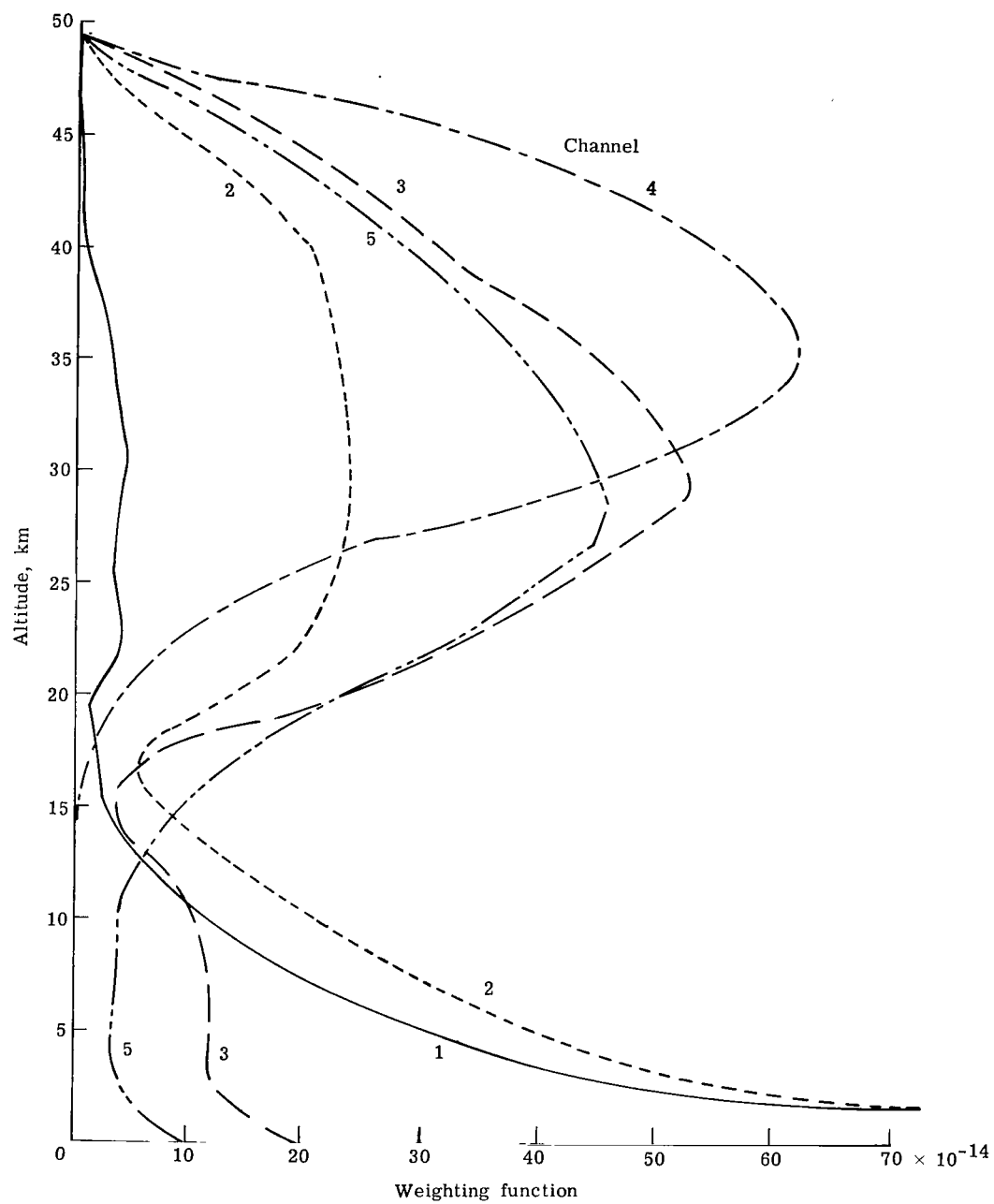


Figure 5.- Set of weighting functions determined by Smith method.

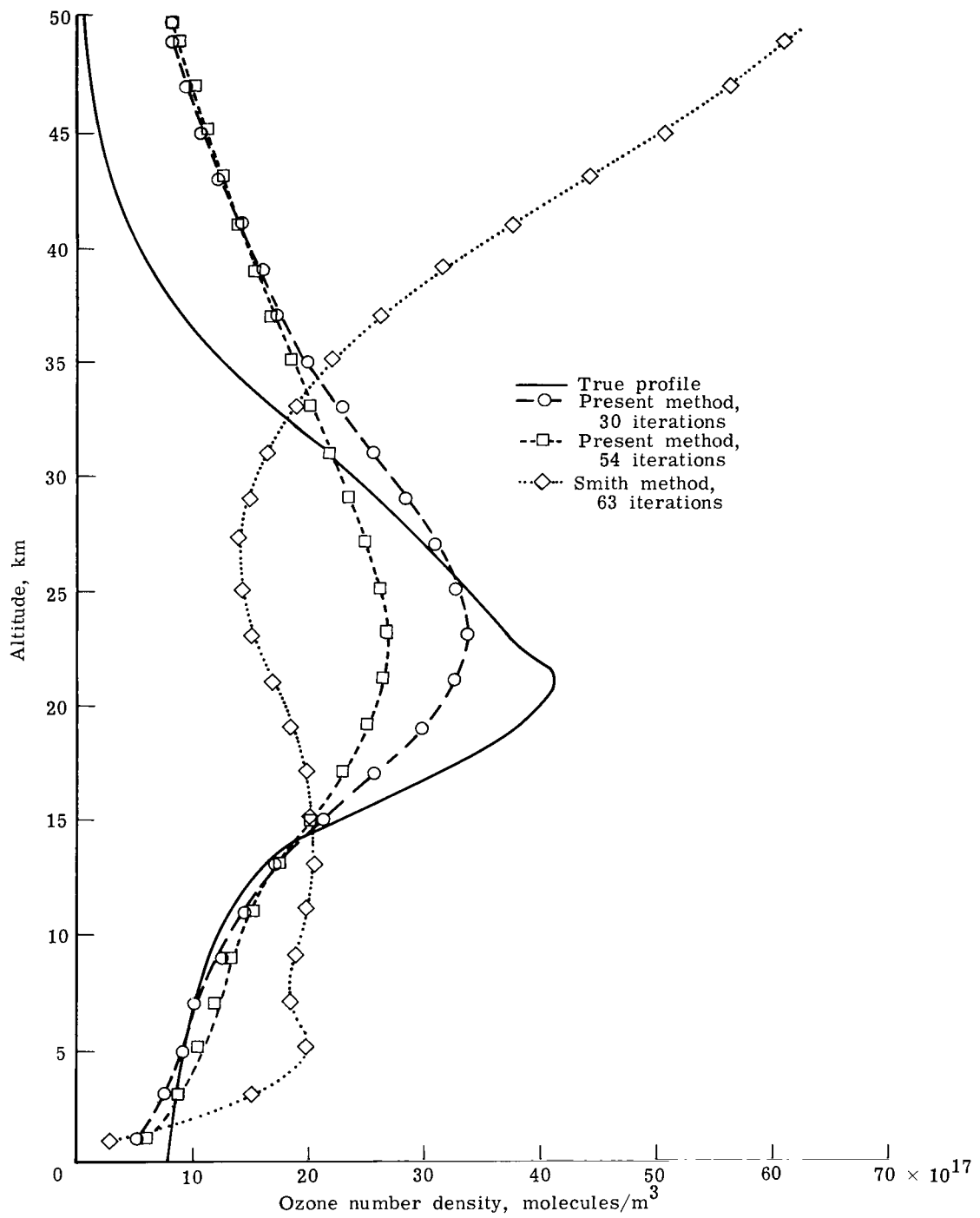


Figure 6.- Results of inversion algorithms at various iteration steps, first demonstration case.

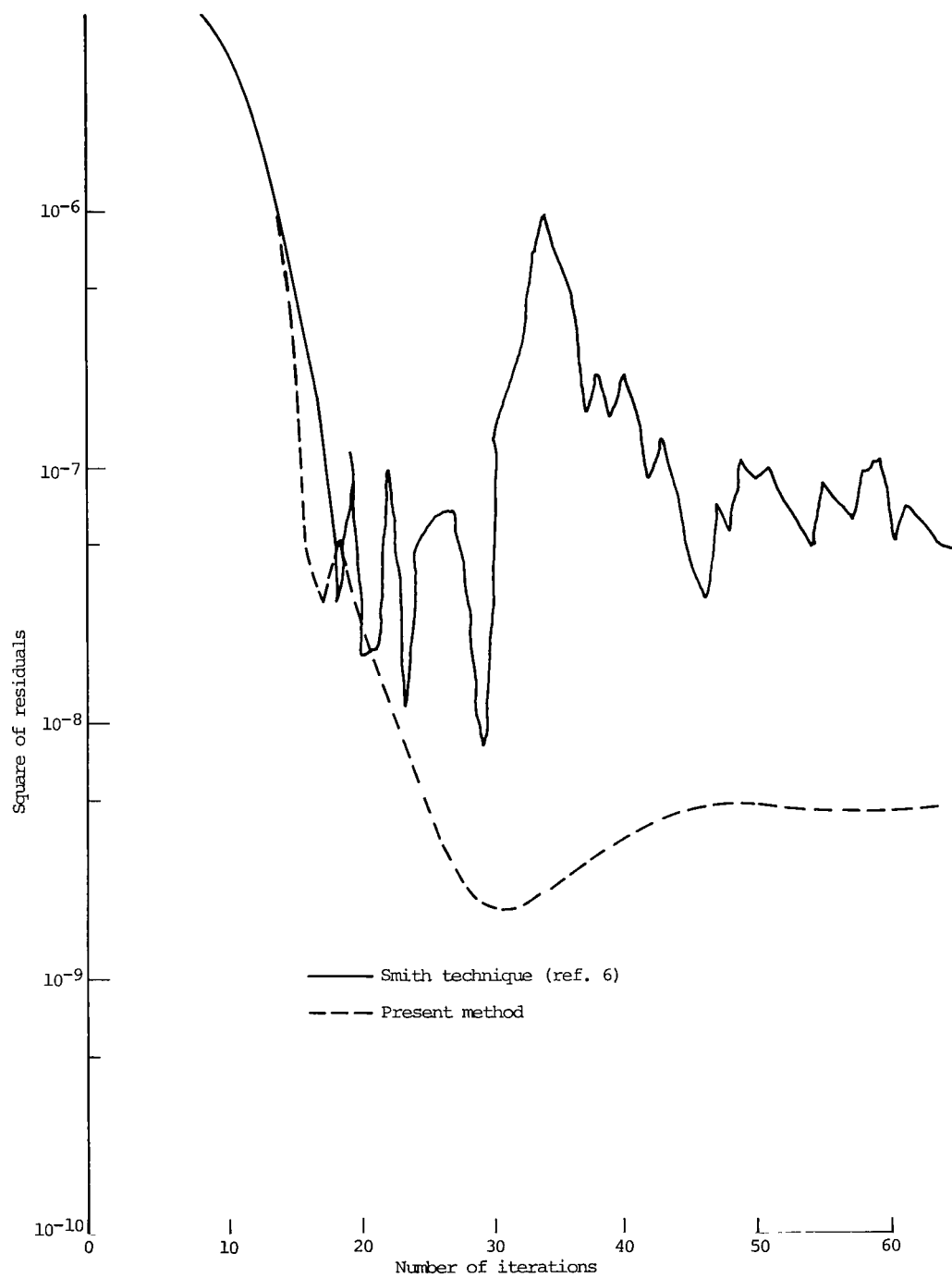


Figure 7.- Residuals for first demonstration case.

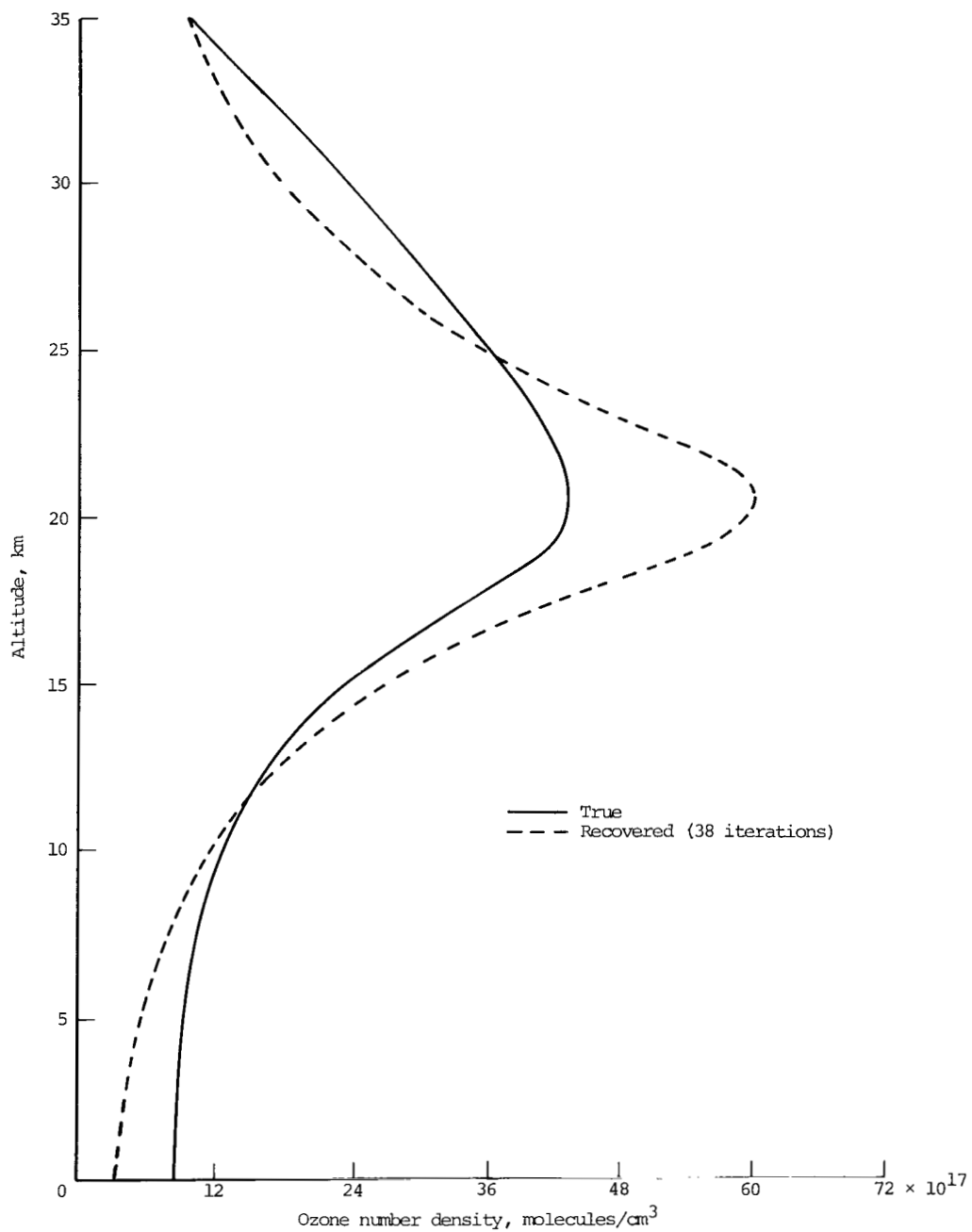


Figure 8.- Profile retrieval using present method for second demonstration case.

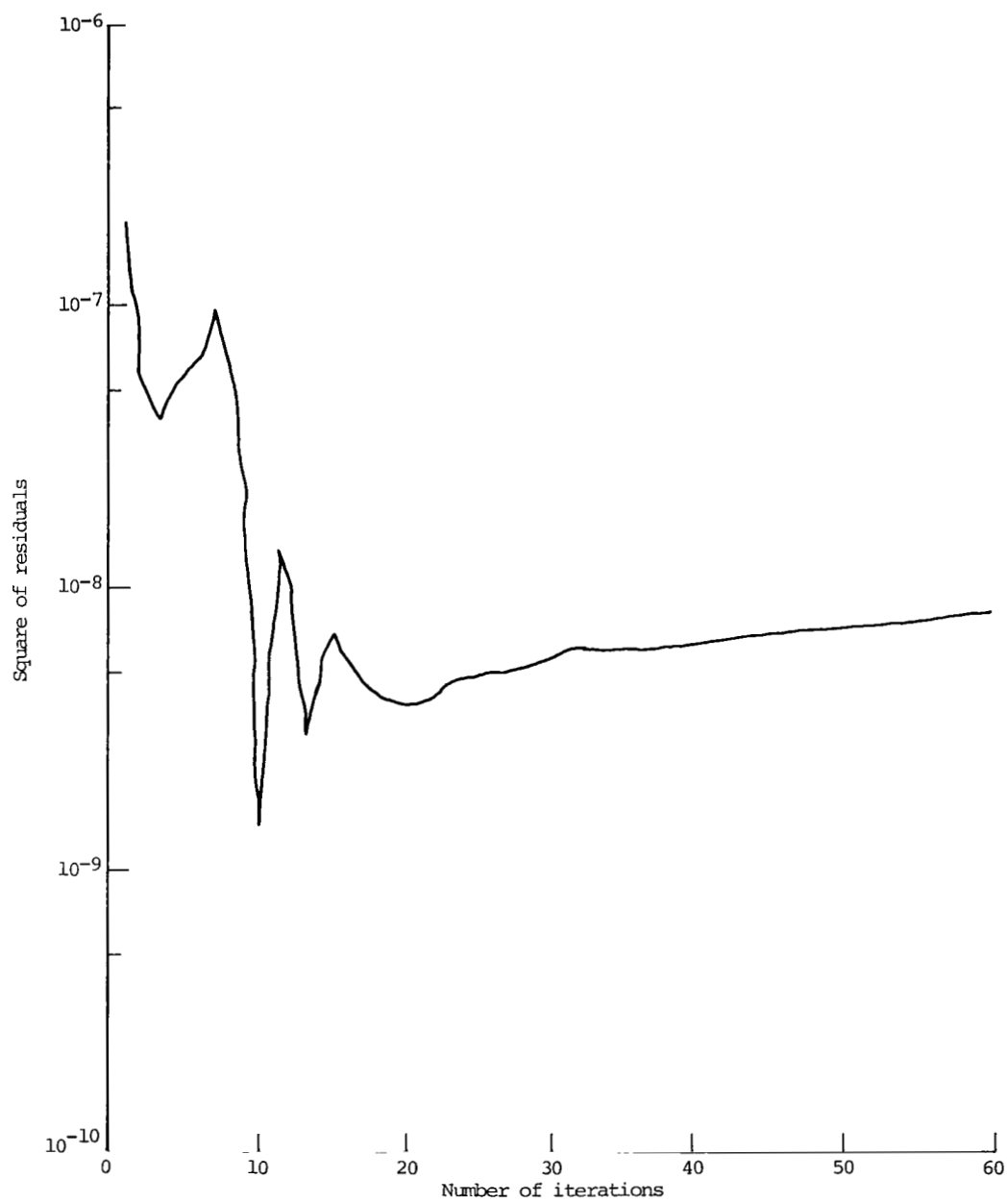


Figure 9.- Residuals for second demonstration case.

1. Report No. NASA TP-1587		2. Government Accession No.		3. Recipient's Catalog No.	
4. Title and Subtitle AN ASYMPTOTIC EXPANSION APPROACH TO THE INVERSE RADIATIVE TRANSFER PROBLEM				5. Report Date December 1979	
7. Author(s) Richard I. Gomberg and James J. Buglia				6. Performing Organization Code	
9. Performing Organization Name and Address NASA Langley Research Center Hampton, VA 23665				8. Performing Organization Report No. L-13165	
12. Sponsoring Agency Name and Address National Aeronautics and Space Administration Washington, DC 20546				10. Work Unit No. 506-61-53-04	
15. Supplementary Notes				11. Contract or Grant No.	
16. Abstract A number of accepted techniques exist to invert radiant transfer data. Each technique involves certain assumptions and has inherent limitations. Derived here is a new iterative technique which recovers density profiles in a nonhomogeneous absorbing atmosphere. The technique is based on the concept of factoring a function of the density profile into the product of a known term and a term which is not known, but whose power series expansion can be found. This series converges rapidly under a wide range of conditions. A demonstration example of simulated data from a high-resolution infrared heterodyne instrument is inverted. For the examples studied, the technique is shown to be capable of extracting features of ozone profiles in the troposphere and to be particularly stable.				13. Type of Report and Period Covered Technical Paper	
17. Key Words (Suggested by Author(s)) Inversion techniques Remote sensing Density profiles				14. Sponsoring Agency Code	
18. Distribution Statement Unclassified - Unlimited				Subject Category 46	
19. Security Classif. (of this report) Unclassified	20. Security Classif. (of this page) Unclassified	21. No. of Pages 29	22. Price* \$4.50		

* For sale by the National Technical Information Service, Springfield, Virginia 22161

NASA-Langley, 1979

National Aeronautics and
Space Administration

Washington, D.C.
20546

Official Business

Penalty for Private Use, \$300

THIRD-CLASS BULK RATE

Postage and Fees Paid
National Aeronautics and
Space Administration
NASA-451



5 1 10, E, 121179 S00903DS
DEPT OF THE AIR FORCE
AF WEAPONS LABORATORY
ATTN: TECHNICAL LIBRARY (SUL)
KIRTLAND AFB NM 87117

NASA

POSTMASTER:

If Undeliverable (Section 158
Postal Manual) Do Not Return